Angewandte Chemie
Eine Zeitschrift der Gesellschaft Deutscher Chemiker

Supporting Information

Modifying the Steric Properties in the Second Coordination Sphere of Designed Peptides Leads to Enhancement of Nitrite Reductase Activity

*Karl J. Koebke, Fangting Yu, Elvin Salerno, Casey Van Stappen, Alison G. Tebo, James E. Penner-Hahn, and Vincent L. Pecoraro**

anie_201712757_sm_miscellaneous_information.pdf

Supporting information

Table of Contents

1. General procedures

All samples containing Cu^{I} were handled in an inert atmosphere box using oxygen-free buffer solution or water. A stock solution of $[Cu(CH_3CN)_4]BF_4$ was prepared in degassed acetonitrile (ca. 0.1 M). $[Cu(CH_3CN)_4]BF_4$ was purchased from Sigma Aldrich and dissolved in degassed acetonitrile to obtain a stock solution (the concentration of which was determined by spectrophotometric titrations using 2,9-dimethyl-1,10-phenantroline).[1] A $CuCl_2$ solution was prepared by $CuCl_2{\cdot}2H_2O$ salt in water (degassed water for activity studies) and the concentration was determined by inductively coupled plasma (ICP) optical emission spectroscopy. Unless otherwise stated, all Cu^{I}(3SCC) and Cu^{II}(3SCC) solutions were prepared by reacting apo-peptides in aqueous solution with $[Cu(CH_3CN)_4]BF_4$ acetonitrile solution or $CuCl_2$ aqueous solution. The pH values were registered using Hamilton glass microelectrodes. UV-visible spectra were collected on a Varian Cary 100 UV-Vis spectrophotometer with a thermostat, using matched quartz cells of 1 cm path length. EPR spectra were recorded on a Bruker EMX X-band EPR spectrometer with a liquid nitrogen cryostat.

2. Peptide synthesis and purification

All peptides in this study were synthesized on an Applied Biosystems 433A peptide synthesizer using standard protocols36 and purified by reverse-phase HPLC on a C18 column at a flow rate of 20 mL/min using a linear gradient varying from 0.1% trifluoroacetic acid (TFA) in water to 0.1% TFA in 9:1 CH_3CN: H_2O as previously reported.[2] Peptides were collected over 27-29 min and characterized by electrospray mass spectrometry. Peptide concentrations were determined based on the tryptophan absorbance at 280 nm (ε = 5500 $M^{-1}cm^{-1}$).[3]

3. Determination of first order rate constants of Cu^{II}(3SCC).

The measurement of the rate of ascorbate oxidation was carried out as previously reported.[4,5] Briefly, 30 mM $NaNO_2$ was mixed with 0.18 mM Cu^{II}(3SCC) and 0.09 mM apo-3SCC (to ensure that over 99% of Cu^{II} is bound to the peptide). The reaction was initiated by adding 6 equivalents of sodium ascorbate (NaAsc) with respect to Cu^{II}. The

consumption of sodium ascorbate (NaAsc) was monitored by UV-Visible spectroscopy. The control was a mixture of 30 mM $NaNO_2$ and 0.09 mM apo-3SCC with the same amount of NaAsc. The rates of the reaction were calculated by two times the different rates of NaAsc consumption (decrease of absorbance at 251 nm, ε = 8250 $M^{-1}cm^{-1}$)[6] between the sample and the control. The first order rate constant was calculated by dividing the rate of the reaction by the concentration of Cu^{II}(3SCC).

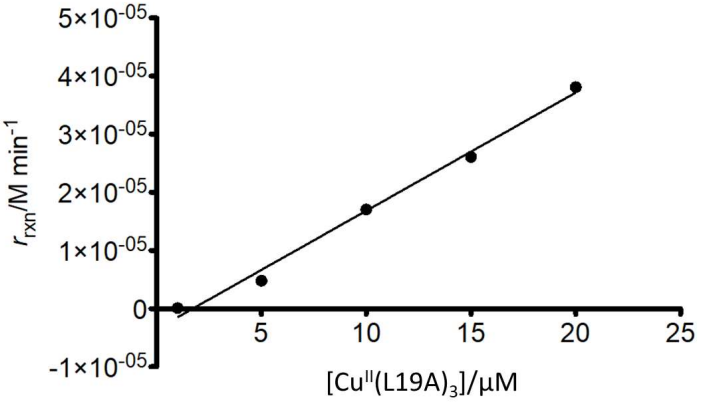

Figure S1. Linear correlation between NiR rate and $Cu^{II}(L19A)_3^{2+}$ concentration.

4. Michaelis-Menten kinetics of $Cu^{II}(L19A)_3^{2+}$.

Different concentrations of $NaNO_2$ (0.5, 1, 2.5, 5, 10, 20, 30, 40, 50, 100, 150, 200, 300 mM) were incubated with the peptides. Samples contained 10 μM Cu^{II}(3SCC), 70 μM apo-peptide in 50 mM potassium phosphate buffer. Controls contained 70 μM apo-peptide. The pH was adjusted to 5.8 by the addition of concentrated KOH. The reactions were initiated by injecting NaAsc to the reaction mixture. The final NaAsc concentration was 1.5 mM. The rates of the reactions were calculated the same way as described above. The rates were correlated to the substrate concentrations through fitting to the Michaelis-Menten equation in Prism 5 (GraphPad software).

Figure S2 shows the Michaelis-Menten kinetics trace of $Cu(L19A)_3$ at pH 5.8. Fitting the data to the Michaelis-Menten equation yielded a v_{max} of 1.42(2) × 10^{-4} M min^{-1} and a K_M of 0.24(5) M. The catalytic efficiency k_{cat}/K_M is 60(15) $min^{-1}M^{-1}$.

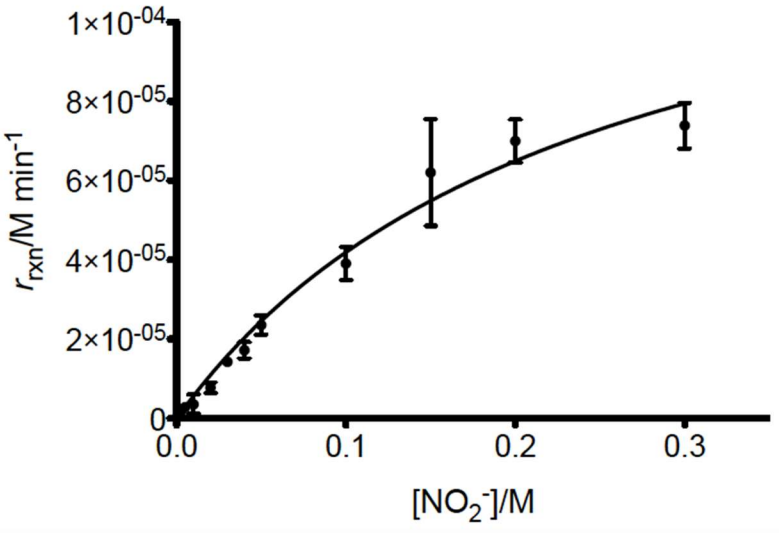

Figure S2. Michaelis-Menten kinetics of Cu(L19A)$_3$ at pH 5.8.

5. pH dependence of k_{1st}' of $Cu^{II}(L19A)_3^{2+}$.

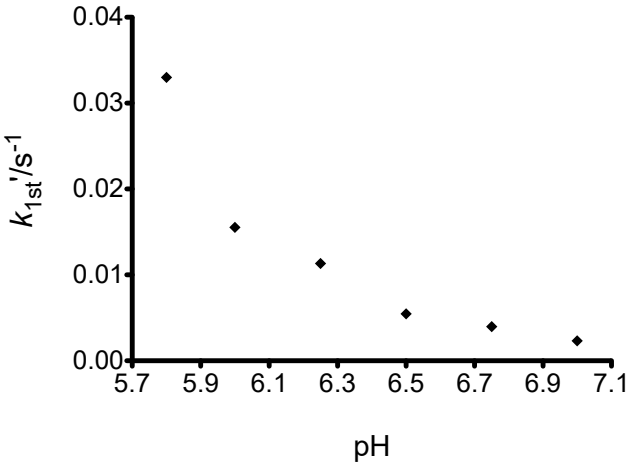

Figure S3. pH dependence k_{1st}' of $Cu^{II}(L19A)_3^{2+}$.

6. XAS sample preparation, data collection, and data fitting

A 1.0 mM $Cu^{I}(3SCC)^{+}$ solution was made in the glovebox with 50 mM degassed buffer (MES for pH 5.8 condition, HEPES for pH 7.4 condition). 1 mM excess apo-3SCC was added to ensure the free Cu^{I} concentration was minimal (< 0.01 %). The samples were mixed with 50 % glycerol as a glassing agent and loaded into a sample cell and

frozen in liquid nitrogen.

Measurements were carried out at Stanford Synchrotron Radiation Lightsource (SSRL) beamline 7-3 with a Si(220) double-crystal monochromator and a flat Rh-coated harmonic rejection mirror. Samples were maintained below 10 K with an Oxford Instruments liquid helium cryostat. Data were measured as fluorescence excitation spectra using a 30-element Ge detector array normalized to incident intensity measured with a N_2 filled ion chamber. Data were measured with steps of 0.25 eV in the XANES region (1 sec integration time) and 0.05 $Å^{-1}$ in the EXAFS region to k = 13.5 $Å^{-1}$ (1~20 sec integration, k^3 weighted). Energies were calibrated by assigning the lowest energy inflection point of a copper metal foil as 8980.3 eV. An initial E_0 value of 9000 eV was used to convert data to k-space, and the background was removed using a 3-region cubic spline. EXAFS data were analyzed using EXAFSPAK[7] and FEFF 9.0.[8] XANES data were normalized using MBACK[9].

Single- and multiple-scattering fitting of EXAFS data were performed using EXAFSPAK[7] with *ab initio* amplitude and phase parameters calculated using FEFF 9.0.[8] An initial model of Cu^I-imidazole coordination was built based on the averaged bond distances reported for the crystal structures of synthetic molecules containing Cu(I)-imidazole constituent.

7. pH-dependent change of Cu^I coordination in $(L19A)_3$ and $(L26A)_3$

The L19A mutation leads to a two-coordinate Cu^I at pH 5.8 while L26A leads to a 3-coordinate Cu^I. The XANES of $Cu^I(L19A)_3^+$ has relatively high intensity at ~8984 eV, typical of a two-coordinate Cu^I center while that of $Cu^I(L19A)_3^+$ is notably less intense typical of a three-coordinate Cu^I center. As pH is increased from 5.8 to 7.4, this feature decreases in $Cu^I(L19A)_3^+$. At pH 7.4, the XANES of $Cu^I(L19A)_3^+$ more resembles that of a three-coordinate Cu^I (Figure S4). The EXAFS fittings of $Cu^I(L19A)_3^+$ at these two pH conditions are consistent with the change of coordination numbers (Figure S5).

At pH 5.8, the bond length of a two-coordinate Cu^I-N_{imid} is 1.86 Å, and we know that the bond length of a three-coordinate Cu^I-N_{imid} in the TRI scaffold is 1.93 Å. For $Cu^I(L19A)_3^+$ at pH 7.4, the bond length is 1.91 Å, which corresponds to a mixture of ~30% two-coordinate and ~70% three-coordinate Cu^I-N_{imid}.

At pH 6.5, by correlating the intensity of the pre-edge features and the bond lengths at pH 5.8 and 7.4, we estimate that the Cu^{I}-N_{imid} bond length at pH 6.5 is 1.88 Å. If we plot these points in a pH-bond length coordinate [(5.8, 1.86),(6.5, 1.88),(7.4, 1.91)], we obtain a pH-bond length correlation: bond length = 0.0313×pH+1.68. Using this correlation, we estimate that at pH 7.0, the bond length should be 1.90 Å, which corresponds to 43% two-coordinate and 57% three-coordinate Cu^{I}.

The XANES and EXAFS of $Cu^{I}(L26A)_3^+$ follow a similar, though less pronounced, pattern with the XANES (Figure S6) decreasing in intensity and EXAFS (Figure S7) showing an increased Cu^{I}-N_{imid} of 1.93 at pH 7.4 compared to a bond length of 1.91 at pH 5.8.

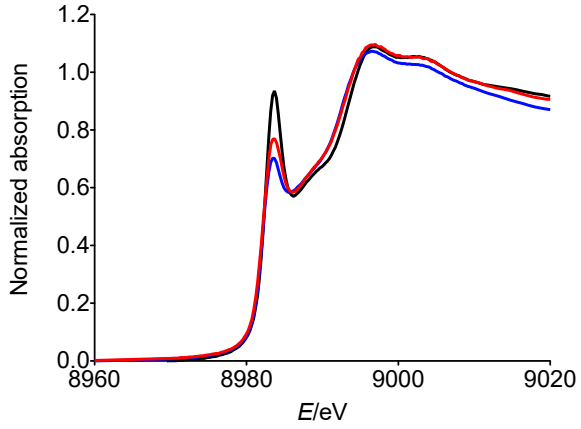

Figure S4. XANES of $Cu^{I}(L19A)_3^+$ at pH 5.8 (black spectrum), pH 6.5 (red spectrum) and pH 7.4 (blue spectrum).

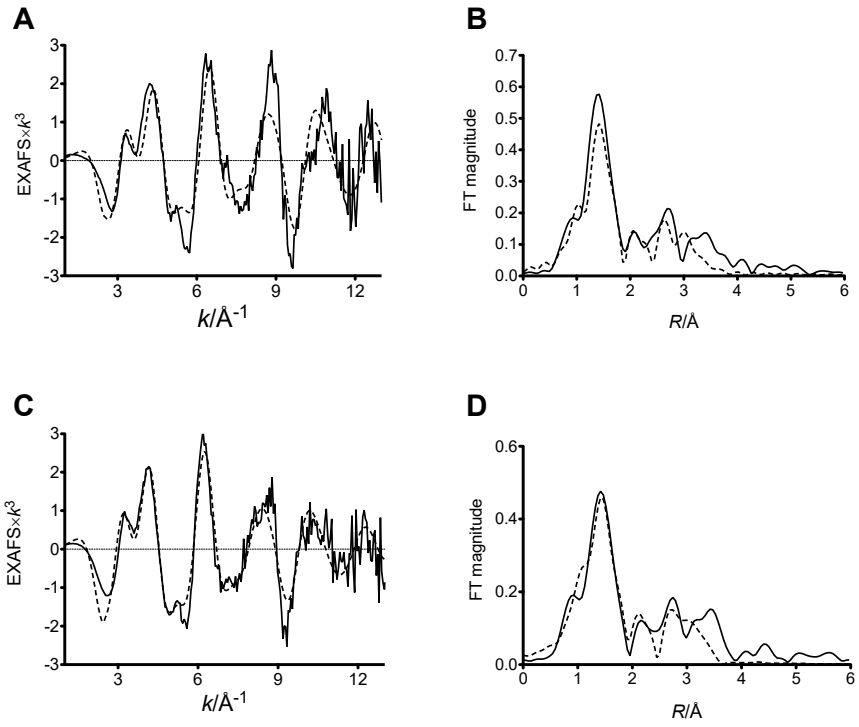

Figure S5. EXAFS of $Cu^{I}(L19A)_3^+$ at pH 5.8 (A) and pH 7.4 (C) and the Fourier transform of the EXAFS at pH 5.8 (B) and pH 7.4 (D). Experimental data are shown as solid lines and fittings are shown as dashed lines.

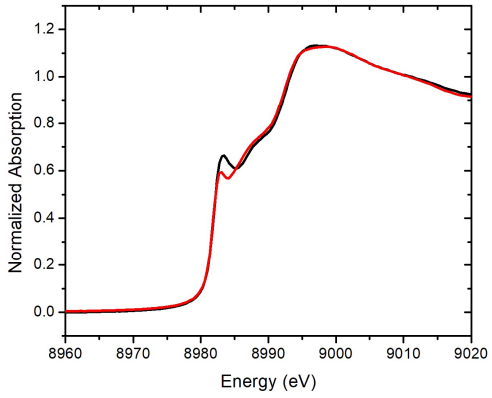

Figure S6. XANES of $Cu^{I}(L26A)_3^+$ at pH 5.8 (black spectrum) and pH 7.4 (red spectrum)

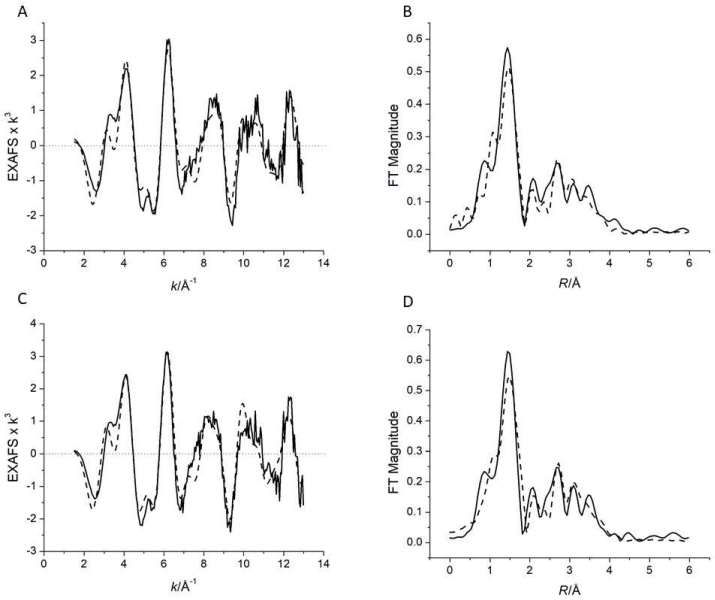

Figure S6. EXAFS of $Cu^{I}(L16A)_3^{+}$ at pH 5.8 (A) and pH 7.4 (C) and the Fourier transform of the EXAFS at pH 5.8 (B) and pH 7.4 (D). Experimental data are shown as solid lines and fittings are shown as dashed lines.

8. EXAFS Fitting Parameters at pH 5.8 for all constructs reported

Construct	Model	Distance (Å)	Debye-Waller 1x10-3	F value
$L19_DL$	$Cu(Imidazole)_2$	1.92	8.09	94
	$Cu(Imidazole)_3$	1.92	9.81	74
L19A	$Cu(Imidazole)_2$	1.86	7.97	95
	$Cu(Imidazole)_3$	1.86	9.69	87
L19D	$Cu(Imidazole)_2$	1.88	7.78	81
	$Cu(Imidazole)_3$	1.88	9.78	77
L26A	$Cu(Imidazole)_2$	1.91	7.98	56
	$Cu(Imidazole)_3$	1.91	10.12	42
L26D	$Cu(Imidazole)_2$	1.91	6.53	61
	$Cu(Imidazole)_3$	1.91	8.64	47

Table S1. EXAFS fitting parameters of 2 and 3 coordinate Histidine complexes for all constructs reported in main manuscript. Only the parameters that were refined are shown. Histidine outer-shell paths are calculated using a rigid imidazole group as a model. Fits were performed using all outer-shell paths.

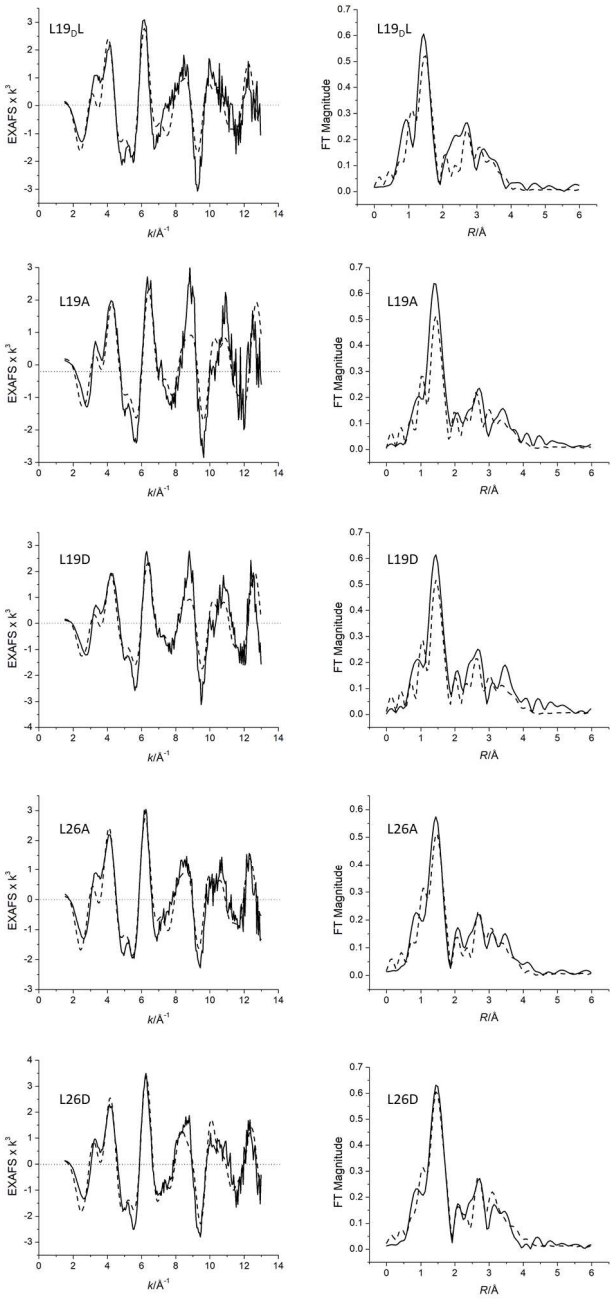

Figure S8. EXAFS and the Fourier Transform of EXAFS for all constructs reported at pH 5.8. Fits were created using the best fit models reported in main manuscript ($Cu^{I}(His)_2$ for L19A and L19D or $Cu^{I}(His)_3$ for $L19_DL$, L26A, and L26D

9. References

[1] M. Meyer, A.-M. Albrecht-Gary, C. O. Dietrich-Buchecker, J.-P. Sauvage, *Inorg. Chem.* **1999**, *38*, 2279–2287.

[2] B. T. Farrer, N. P. Harris, K. E. Valchus, V. L. Pecoraro, *Biochemistry* **2001**, *40*, 14696–705.

[3] J. M. Walker, Ed. , *The Protein Protocols Handbook*, Humana Press Inc., Totowa, NJ, **2002**.

[4] M. Tegoni, F. Yu, M. Bersellini, J. E. Penner-Hahn, V. L. Pecoraro, *Proc. Natl. Acad. Sci. U. S. A.* **2012**, *109*, 21234–9.

[5] F. Yu, J. E. Penner-Hahn, V. L. Pecoraro, *J. Am. Chem. Soc.* **2013**, *135*, 18096–18107.

[6] M. I. Karayannis, D. N. Samios, C. H. P. Gousetis, *Anal. Chim. Acta* **1977**, *93*, 275–279.

[7] G. N. George, *EXAFSPAK* **2000**.

[8] A. Ankudinov, J. Rehr, *Phys. Rev. B* **1997**, *56*, R1712–R1716.

[9] T.-C. Weng, G. S. Waldo, J. E. Penner-Hahn *J. Synch. Rad.* **2005**, 12, 506-510